2 Stellar Energy Generation – PP-chain physics

2.1 The PPI chain and energetics

Figure 3 shows the main sequences by which hydrogen nuclei (protons) are converted into helium nuclei. The first step is the weak interaction process of Eq. 3. This step determines the rate of energy production in MS stars, and this property is the focus of the next two sections. Here, we look at the overall energetics of the processes.

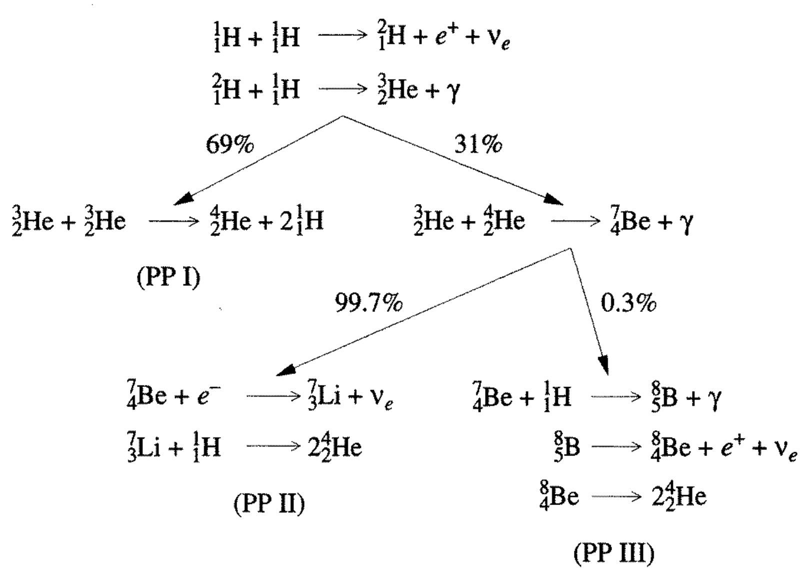

Figure 3: The PP chains. (Figure 10.8 of Carroll and Ostlie.)

All three of the PP chains involve conversion of 4 protons to a helium-4 nucleus. Reference to 1 shows that ^4_2He is unusually stable relative to isotopes of similar atomic mass. In fact, ^4_2He is also known as an alpha particle, and due to its large binding energy and stability, is a typical by-product of nuclear reactions such as fission. Figure 3 shows a branching ratio of 69% for process 3 of the PPI chain. This reflects the probability of this path. However, the PPI chain accounts for 85% of the overall rate of ^4_2He production, and hence about 85% of the total energy output of the sun and similar MS stars. So we use the PPI chain to illustrate energy production, and in so doing we account for the vast majority of the solar luminosity.

Rewriting the PPI chain:

$$\begin{aligned} {}^1_1H + {}^1_1H &\to {}^2_1H + e^+ + \nu_e \\ {}^2_1H + {}^2_1H &\to {}^3_2He + \gamma \\ {}^3_2He + {}^3_2He &\to {}^4_2He + 2{}^1_1H \end{aligned} \tag{4}$$

We note that process 3 requires two reactions each of processes 1 and 2. So in sum there are 6 protons reactants and 2 proton products. Hence, the net effect of the PPI chain in terms of overall energetics is equivalent to:

$$4{}^1_1H \to {}^4_2He + 2e^+ + 2\nu_e + 2\gamma \ . \tag{5}$$

We follow the usual practice in nuclear physics of using the *atomic mass unit*, or u for the rest masses of nuclei. By definition,

$$1u = \frac{1}{12} M({}^{12}_6C) \ ,$$

and a conversion to MeV can be made from Section 1.2. Using the AMU, the proton mass is 1.0078 u and the ${}^4_2He$ mass is 4.0026 u. So the energy available to the other final state particles, both as rest energy and kinetic energy, is

$$\Delta m = [4 \times 1.0078 - 4.0026] = 0.0287 \text{ u} \ ,$$

or $\Delta mc^2 = 0.0287 \times 931.49432$ MeV/u $= 27$ MeV. The positron rest mass will be available for kinetic energy, too, since it will annihilate with an ambient electron. So except for the energy given to the neutrinos, which exit the star without depositing any energy, the 27 MeV is available to provide the solar luminosity. (The neutrinos will be discussed separately in lecture 6.) We note that the first step of the PP chain, the *p*-*p* interaction, provides only about 0.3 MeV of kinetic energy.

So for each PPI reaction (*i.e.* for every 4 protons), the fraction of stellar mass which is converted to energy luminosity is (except for the neutrinos)

$$\epsilon = 0.0287/4.0313 \approx 7 \times 10^{-3} \tag{6}$$

Hence, the *available* hydrogen mass can be eventually converted into energy with an efficiency of 0.7%.

2.2 The pp interaction: Coulomb barrier penetration

The strong force for the *n*-*p* and *p*-*p* interactions are identical. (This is a symmetry property called *isospin*.) But we now have to add to this the Coulomb interaction between the protons:

$$U(r) = U_{\text{strong}} + U_{\text{coulomb}}\ ,\ \ U_{\text{coulomb}} = \frac{1}{4\pi\epsilon_0}\frac{e^2}{r}\quad \text{(SI)}$$

This potential is depicted in Figure 4.

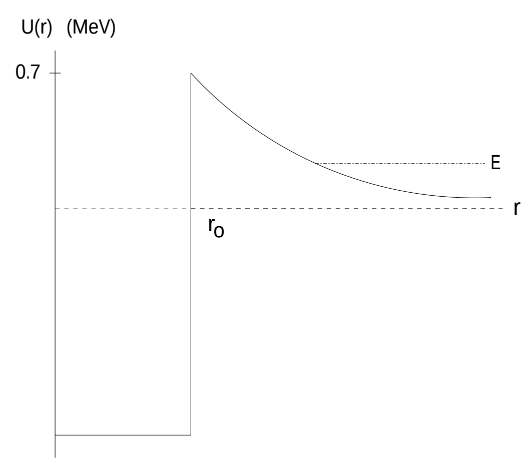

Figure 4: Potential energy model of the proton-proton interaction.

At $r = r_0 = 2$ fm we have (using SI units, then converting to eV):

$$U_{\text{coul}} = \left[(9\times 10^9)(1.6\times 10^{-19})^2/(2\times 10^{-15})\right]\times 1\,\text{eV}/1.6\times 10^{-19}\ \text{J} = 0.7\ \text{MeV}$$

So while the Coulomb barrier is 0.7 MeV, the average kinetic energy of the protons, from Equation 1 is ≈ 1 KeV. So classically, a proton at this average energy will never be able to get close enough to another proton to engage in strong or weak interactions. However, quantum mechanics provides the possibility of barrier penetration. We now sketch the solution to this calculation, which will be familiar to students who have had an introductory quantum course.

In the case of a 1-dimensional step potential of height U_b and width L, a particle of mass m and kinetic energy E has a barrier penetration probability P_G in the case where $E \ll U_b$ of $P_G \approx e^{-\gamma}$, where $\gamma^2 = 8mL(U_b - E)/\hbar^2$. For our potential of Fig. 4, where we assume spherical symmetry, we have an analogous solution to the 1-dimensional step potential, except that we now have to integrate over the Coulomb potential. So U_b is replaced by a geometrical factor multiplied by the barrier height. In the limit $E \ll$ 0.7 MeV, which is our situation, the solution for the barrier penetration probability becomes

$$P_G dE \approx e^{-\gamma} dE \ , \quad \gamma^2 = E_G/E \ , \tag{7}$$

where E_G, known as the Gamow energy, depends on the composition of the charged-particle gas. In the present case for protons, this is

$$E_G = (2\mu_m/\hbar^2)\left[\frac{e^2}{4\epsilon_0}\right]^2 \tag{8}$$

in SI units, where μ_m is the classical reduced mass of the p-p system, $m_p/2$. The factor 1/4 comes from the integral over the Coulomb barrier. Using combinations defined in Section 1.2 gives

$$E_G = \frac{1}{8}\frac{m_p c^2}{\hbar^2 c^2}(4\pi\hbar c\alpha)^2 = (938 \text{ MeV})\left(\frac{\pi}{137}\right)^2 = 0.49 \text{ MeV}$$

Therefore, for an average proton kinetic energy of $\frac{3}{2}kT = 1$ KeV, we find the Coulomb barrier penetration probability to be

$$P_G \approx e^{-\sqrt{490/1}} \approx 10^{-10} \tag{9}$$

One can compare the probability above with that for which the protons exceed the classical Coulomb barrier because there is a small fraction which have thermal energies far above the average. For a classical, non-interacting gas the distribution of kinetic energies at a temperature T is given by the Maxwell-Boltzmann distribution:

$$P_{mb}(E)dE \propto E^{1/2}e^{-E/kT}dE \tag{10}$$

which follows the exponential decay form far above the average. For $kT \approx 1$ KeV, the probability of finding a proton at the Coulomb barrier is $\propto e^{-720}$

compared to the quantum barrier penetration factor which we found to be $\propto e^{-22}$. Clearly the thermal mechanism is insignificant compared to quantum tunneling in this case.

A correct determination of the probablility of Coulomb barrier penetration should involve the convolution of the two distributions, of the form:

$$P_G(E) = \int_0^\infty P_q(E')P_{mb}(E-E')dE' \tag{11}$$

The resulting distribution, called the Gamow curve, has a maximum at about 5 KeV for a star like our sun.

2.3 Proton survival time

We can now estimate the rate of the initial hydrogen-burning process given in Equation 3. As stated earlier, this process is the slowest in the PP chain, and hence determines the rate of energy production in main-sequence stars. This rate is given by

$$R_{pp} = R_{\text{col}} P_G P_{pn} \tag{12}$$

where R_{col} is the pp collison rate, P_G is the barrier penetration probability of Equation 11, and P_{np} is the probability that a barrier penetration results in the weak process $p \to n + e^+ + \nu$.

In class, we estimated the collision rate using the standard formulation $R_{\text{col}} = nv\sigma$, where n is the number density of protons, v is their average speed, and σ is the collision cross section. n is about 10^{26} cm^{-3}. We can find v from $\frac{3}{2}kT = \frac{1}{2}mv^2 = \bar{E} \approx 1$ KeV, which gives $(v/c)^2 = 2\bar{E}/(mc^2) = 2/9.38 \times 10^5$, so $v \approx 4 \times 10^7$ cm/s. And we find σ from the proton scattering radius (~ 1 fm, giving $\sigma \sim 10^{-26}$ cm^2. So then we have

$$R_{\text{col}} \approx (10^{26})(4 \times 10^7)(10^{-26}) \sim 4 \times 10^7 \text{ s}^{-1}$$

Because the weak force has such a short range, its strength is very small relative to the strong force for the rather large deBroglie wavelengths ($\lambda = h/p$) associated with the 1 KeV protons in the stellar cores. Therefore, even after a proton manages to penetrate the Coulomb barrier of the other proton, it is very unlikely that the weak process we need will occur rather than p-p elastic scattering via the strong interaction. Hence, we need to estimate

$$P_{pn} = P(p \to n + e^+ + \nu)/P(pp \to pp)$$

. We are now going to *revise and reformulate* the expression in Equation 12 compared to what was done in class in order to fill in the pieces more easily. We note that since the collision is dominated by strong *p*-*p* scattering at these energies, then $P_{pp} \approx P_{\rm col}$. Furthermore, $P_{\rm pn} = \Gamma_{pn}/\Gamma_{pp}$, where Γ is the transition rate (transition probability per unit time). Hence, we can re-write Eq. 12 as

$$R_{pp} = R_{\rm col} P_G P_{pn} = N\Gamma_{pp} P_G(\Gamma_{pn}/\Gamma_{pp}) = N P_G \Gamma_{np} \tag{13}$$

where N is the number of protons available for the *pp* process. Now the rate for the weak β decay process can be used to evaulate Γ_{np}. It is a standard nuclear/particle calculation (see for example Halzen and Martin (1984)):

$$\Gamma = \frac{G^2}{\hbar\pi^3}\int_0^{E_0} p^2(E_0 - E)^2 dp\ , \tag{14}$$

where p and $E = \sqrt{p^2 + m_e^2}$ are the daughter electron's momentum and energy ($c \equiv 1$ momentarily), and E_0 is the binding energy difference between final and initial nuclei. (This calculation ignores many details, but should provide an order of magnitude estimate.) G is the Fermi (or weak) constant, which is related to the strength of the weak force: $G/(\hbar c)^3 = 1.2 \times 10^{-5}$ GeV^{-2}. An evaluation of the integral in the expression above is shown in Figure 5 as a function of E_0. The relativistic approximation $p \gg m_e c$ often shown in texts is clearly not appropriate for binding energies of the *p*-*p* reaction. Using $E_0 = 0.3$ MeV for the *p*-*p* process, Eq. 14 yields $\Gamma \sim 10^{-7}$ s^{-1}. Combining this with the Coulomb barrier penetration probability Eq. 9, we find

$$R_{pp} \sim (N)(10^{-17})\ {\rm s}^{-1}$$

Therefore, our order of magnitude calculation yields an average lifetime for protons in the core of solar-like MS stars of

$$\tau_p = N/R_{pp} \sim 10^{17}\ {\rm s}$$

or about 10 billion years, which is the appropriate time scale. Along with the overall energy output for the PPI chain found in the previous section, we now have a viable model for MS star energy generation.

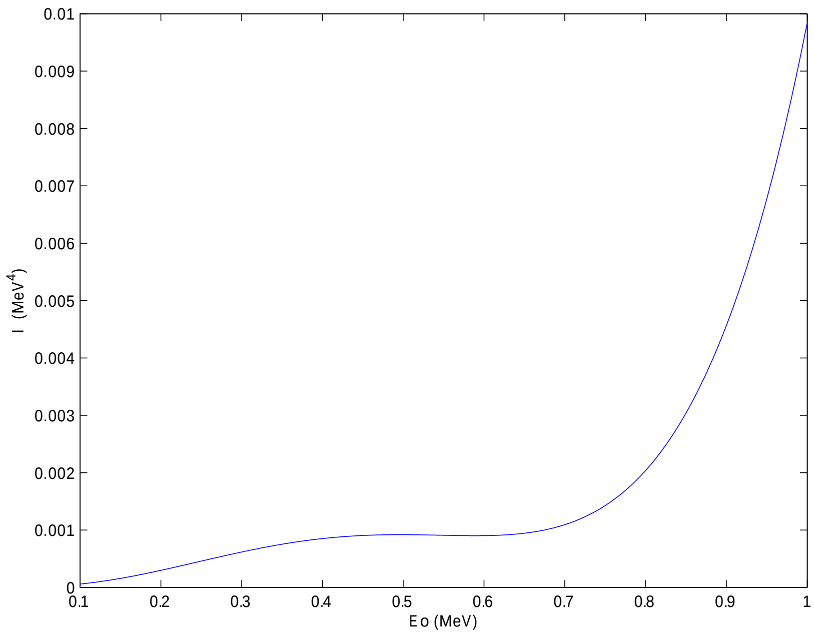

Figure 5: The integral in Eq 14 as a function of E_0.

2.4 Other nuclear sequences

As discussed in Carroll and Ostlie, the temperature dependence of the PP chains is roughly given by $R_{pp} = \alpha_{pp}(T/10^6)^4$, where α depends on many other parameters. Other nuclear fusion processes are also possible. One example is the CNO cycle, depicted in Fig. 6.

Typically, these processes involve heavier nuclei, and the temperature dependence is much greater than the PP chain. For example, $R_{cno} = \alpha_{cno}(T/10^6)^{20}$. Two other chains, with even greater temperature dependence, are depicted in Figs. 7 and 8. The latter only becomes relevant for $T \sim 10^9$ K. The basic scenario for how these other chains come into play is as follows. For solar-like MS stars with a core temperature $\sim 10^7$ K. At this temperature, the PP rate dominates the rate, as expected. The higher-A processes have much lower rate at these temperatures, so represent a small correction to energy and element production. Now, since the equation of state gives a pressure $P \propto T$, in the steady state of hydrogen burning the PP will continue to dominate.

$$
\begin{aligned}
{}^{12}_{6}\mathrm{C} + {}^{1}_{1}\mathrm{H} &\rightarrow {}^{13}_{7}\mathrm{N} + \gamma \\
{}^{13}_{7}\mathrm{N} &\rightarrow {}^{13}_{6}\mathrm{C} + e^{+} + \nu_e \\
{}^{13}_{6}\mathrm{C} + {}^{1}_{1}\mathrm{H} &\rightarrow {}^{14}_{7}\mathrm{N} + \gamma \\
{}^{14}_{7}\mathrm{N} + {}^{1}_{1}\mathrm{H} &\rightarrow {}^{15}_{8}\mathrm{O} + \gamma \\
{}^{15}_{8}\mathrm{O} &\rightarrow {}^{15}_{7}\mathrm{N} + e^{+} + \nu_e \\
{}^{15}_{7}\mathrm{N} + {}^{1}_{1}\mathrm{H} &\rightarrow {}^{12}_{6}\mathrm{C} + {}^{4}_{2}\mathrm{He}.
\end{aligned}
$$

Figure 6: The main branch CNO chain. (Equation 10.51 of Carroll and Ostlie.)

However, as hydrogen is depleted the PP pressure is reduced, allowing further gravitational contraction, in turn requiring larger pressure to maintain mechanical equilibrium with a correspondingly larger T. The larger T rapidly increases the rate of the higher-A processes. So as the lighter nuclei are consumed, the burning of these elements will continue at layers ar larger radius, while the inner core will involve the processes with heavier nuclei. These larger rates will consume the fuels relatively quickly. At some point in this evolution, electron degeneracy becomes important. This will be discussed in subsequent lectures.

$$
{}^{12}_{6}\mathrm{C} + {}^{12}_{6}\mathrm{C} \rightarrow
\begin{cases}
{}^{16}_{8}\mathrm{O} + 2\,{}^{4}_{2}\mathrm{He} & *** \\
{}^{20}_{10}\mathrm{Ne} + {}^{4}_{2}\mathrm{He} & \\
{}^{23}_{11}\mathrm{Na} + p^{+} & \\
{}^{23}_{12}\mathrm{Mg} + n & *** \\
{}^{24}_{12}\mathrm{Mg} + \gamma &
\end{cases}
$$

Figure 7: Another high-temperature fusion process. (Equation 10.59 of Carroll and Ostlie.)

$$^{16}_{8}\mathrm{O} + {}^{16}_{8}\mathrm{O} \rightarrow \begin{cases} ^{24}_{12}\mathrm{Mg} + 2\,{}^{4}_{2}\mathrm{He} & * \\ ^{28}_{14}\mathrm{Si} + {}^{4}_{2}\mathrm{He} \\ ^{31}_{15}\mathrm{P} + p^{+} \\ ^{31}_{16}\mathrm{S} + n \\ ^{32}_{16}\mathrm{S} + \gamma \end{cases}$$

Figure 8: Yet another high-temperature fusion process. (Equation 10.60 of Carroll and Ostlie.)